Key Engineering Materials
ISSN: 1662-9795, Vol. 984, pp 63-69
doi:10.4028/p-x4ecaA

Submitted: 2023-09-30
Revised: 2024-05-01
Accepted: 2024-05-02
Online: 2024-08-22

Plasmonic Ag Nanoparticles on SiC for Use as SERS Substrate and in Integrated Optical Sensors for Bio-Chemical Applications

V. Cantaro[1,2,a], A. Sciuto[1,b], A. Brancato[2,c], G. Compagnini[2,d] and G. D'Arrigo[1,e]

[1]Consiglio Nazionale delle Ricerche, IMM, Catania I, 95121, Italy

[2]Department of Chemical Sciences, University of Catania, A. Doria 6, 95125 Catania, Italy

[a]valentina.cantaro@phd.unict.it, [b]antonella.sciuto@imm.cnr.it, [c]antonio.brancato@phd.unict.it, [d]gcompagnini@unict.it, [e]giuseppe.darrigo@imm.cnr.it

Keywords: Plasmonics, Silver Nanoparticles, SiC, Thermal Dewetting, SERS Effect, Optical sensor.

Abstract. Development of optical chemical sensors for the detection of specific toxic chemicals at ultratrace levels and analysis of complex mixtures is crucial for new green and safe technologies [1, 2]. Metallic structures confined at the nanoscale acquire interesting properties such as strongly localizing E fields on their surfaces through Plasmonic Resonance under stimuli of light at certain wavelengths. This nanostructures are called plasmonic structures [3–5]. This effect is exploited to amplify the optical signal obtained by the molecules of interest, located near plasmonic structures [3, 6]. Purpose of the work is the development of innovative, easy to manufacture and cheap optical active layer consisting of Plasmonic Ag Nanoparticles on a Wide Band Gap semiconductor material such as Silicon Carbide to be used as substrate for Surface Enhanced Raman Scattering or for the fabrication of integrated optical sensor for remote chemical and biological applications. In this contest, the phenomenon of Ag thin film thermal dewetting on SiC substrate was implemented to develop a simple nanoparticles synthetic approach. Scanning Electron Microscopy confirmed the formation of Ag nanoparticles by thermal annealing of thin silver film. 4-MBA was used as probe molecule for SERS phenomenon investigation. The formation of a covalent bond between the silver nanostructures, acting as plasmonic "hot spots", and the species of interest enable its detection at very low concentrations, in the range of 10^{-5} M or less, in both Raman and UV-Vis configurations.

Introduction

When Electromagnetic Field of light radiation of appropriate wavelength (λ) interacts with noble Metal Nanoparticles (MNPs) of a size comparable to λ, it induces a collective oscillation of surface conduction electrons called Surface Plasmons (SPs) [3–6]. This results in an electric dipole due to the accumulation of negative charge on one side and positive charge on the opposite side of the nanoparticles (NPs), which in turn produces an electric field, opposite to that of light, leading to a resonant oscillation of conducting electron density at a typical frequency called plasmonic frequency (ω). Thus, a significant electric field enhancements near the NP surface is achieved, decaying rapidly with distance [6, 7]. This phenomenon has been extensively exploited in sensing field because it allows the detection of traces of substances or even single molecules [8–10]. Light that interacts with NPs can be either adsorbed or scattered so, it is possible to define an absorption cross-section and a scattering cross-section. The sum of these two quantities is the so-called extinction cross-section (σ) and represents the particles efficiency to remove photon from incident light, either by scattering or absorption. The amplitude of ω may be evaluated by means of σ. The value of σ for an ideal opaque particle is its geometrical section. But for noble MNPs σ are 10% higher than their geometrical cross-section [7]. The intensity of light passing through the NPs decays exponentially with σ, as shown in Eq. 1:

$$I(x)=I_0e^{-C\sigma d}. \quad (1)$$

Where I_0 is the intensity of incident light, C the concentration of NPs, d is the distance travelled in medium. So, little increase in σ corresponds to great enhancement of absorption [11]. Plasmonic NPs

are also highly sensitive to small changes in refractive index. It is therefore conceivable that, small quantities of the chemical species, adsorbed onto a plasmonic substrate, produced appreciable variations in its absorption spectrum.
Another important application is in Surface Enhanced Raman Scattering (SERS), an analytical tool that has been continuously expanding its range of applications, including biosensing, medicine, environmental monitoring, food safety, and catalysis [12–14]. SERS not only provides an ultra-sensitive analysis strategy to molecular levels, but also produces the "fingerprint" of the target species by effectively enhancing the cross section of Raman spectroscopy, which has high molecular specificity but is intrinsically weak [15-17]
The purpose of the work is to design an innovative, cheap and simple sensing platform consisting of Ag NPs deposited on a Wide Band Gap (WBG) semiconductor material such as Silicon Carbide (SiC) to be used as a substrate for SERS or integrated into a portable device for optical sensor applications. To do this, Solid-State Dewetting (SSD) of metal thin films was exploited as tool for the easy and cheap development of Ag NPs on SiC. The morphological transformation of a continuous thin film into islands or droplets is achieved by a thermal process at temperatures at which the mobility of the constituent atoms begins to be sufficiently high. The driving force behind the SSD is the minimization of surfaces energy of the films and the interface energy between the film and the substrate [18]. SSD occurs at temperatures lower than the metal film melting temperature. Therefore, it can often be an undesirable phenomenon, especially in the field of integrated circuits, since this transformation limits their reliability, particularly when high temperature operation is required [18, 19]. However, for several years it is commonly used to make metal particle arrays [20].

Experimental Section

Materials and Methods. Samples of 1 cm^2 area were prepared using a 300 μm thick Si-terminated 4H-SiC n-type substrate. Ag thin films were deposited on SiC using an ElettroRava thermal evaporator, with a deposition pressure in the chamber of 10^{-8} mbar in pre-deposition asset and of 10^{-6} mbar, during the deposition phase. Ag pellet with a purity of 99,999% were taken. Evaporated thickness was measured by a quartz microbalance system MAXTEK, model TM-350. For Ag NPs Enhancement Factor (EF) determination, 4-mercaptobenzoic acid (4-MBA), purchased from Sigma-Aldrich, was used as standard molecule. Starting from a 0,1 M mother solution concentration, a 4-MBA solution to 10^{-5} M was prepared. Substrates were optically and chemically characterized by UV–VIS spectroscopy (Cary V60) and by confocal Micro-Raman spectrometer (WITEC Alpha r100), with laser wavelengths of 532 nm, at power of 140 μW. Each spectrum was acquired using an integration time of 10". Morphological and structural characterization were performed by Scanning Electron Microscopy (SEM) using an e-beam lithography apparatus Raith 150 in scanning operation mode

Plasmonic Substrate Fabrication. In order to fine-tune the annealing parameters that influence the Dewetting phenomenon of the Silver film, several tests were first carried out by varying thickness of Ag film, annealing temperature (T) and time (t). From the results obtained, not discussed in this work for brevity, we decided to set the annealing parameters at 10 minutes and 200 °C, and the film thickness between 15 and 20 nm. Process was conducted as follows: on a substrate 4H-SiC, a silver film with nominal thickness of 16.6 nm was thermally evaporated. The thermal dewetting were conducted in N_2 ambient at a pressure of 0,86 bar.

Results and Discussion

SEM images at different magnifications (Mag.) are shown in figure 1. Fig. 1a) reports the SEM image (Mag. = 50 KX) of the as deposited silver film that appears in not uniform light grey, evidencing the grains of the polycrystalline film itself from which the dewetting process begins. Fig. 1b) shows the SEM image (Mag. = 10 KX) of the sample after undergoing the annealing process. In this case, the Ag NPs are clearly distinguishable (in light grey color) over the substrate which appears in dark grey.

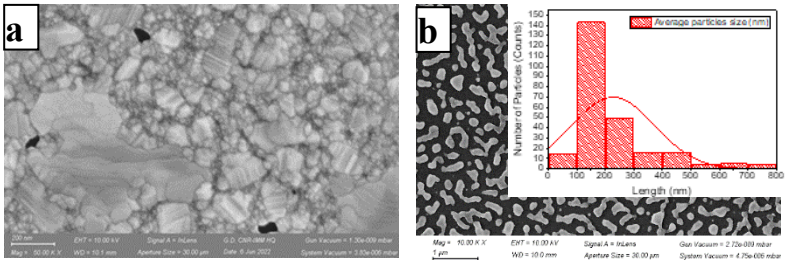

Fig. 1 Scanning Electron Microscopy images of: a) Ag film as deposited on 4H - SiC substrate by Thermal Evaporation; b) Ag NPs formed as a result of thermal dewetting of the silver thin film.

Fig. 1 b) shows the Ag nanoparticles which exhibit an elongated and irregular shape. The dewetting process is in fact a stochastic phenomenon, leading to fabrication of particles with uncontrolled shape and relative positions through a mechanism that proceeds in several steps, including the formation, growth and coalescence of voids [21]. The morphology of NPs obtained by dewetting and their degree of surface coverage are driven by the involved surface energies widely described by Giermann et al. in ref. 22.. In our case, in which the SiC is Si-terminated, a partial wettability was obtained from the dewetting of the Ag thin film [23]. The size distribution evaluation of the NPs was performed using the ImageJ software to analyze the SEM image. The graph of the average NPs size distribution in the x-y plane is shown in the inset of Fig. 1 b. Most Ag NPs are between 100 and 200 nm in size, while the average size distribution is between 150 and 250 nm. ImageJ also provides the degree of surface coverage, which is 43.6 % for NPs. To assess the plasmonic characteristics of NPs, SERS and UV-Vis spectroscopy were performed using 4-MBA as target molecule, a compound widely used for SERS monitoring, consists of a carboxylic group and a hydrogen sulphide group in para to a benzene ring [24]. To bind target molecules to the plasmonic substrate, it was immersed in a 4-MBA solution in ethanol at a concentration of 10^{-5} M for 24 hours, depending on the analyte concentration, on which the kinetics of the chemisorption process of 4-MBA on Ag depends [22-24]. After, substrate was taken out from the solution, rinsed in ethanol and dried in N_2 flow. SEM images of Ag NPs on SiC sample after dipping in 4-MBA solution are shown in Fig. 2, that clearly shows the presence of 4-MBA molecules (dashed red square).

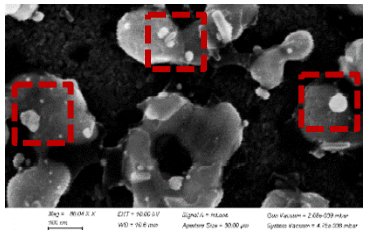

Fig. 2 SEM image of Ag NPs on SiC after dipping in 4-MBA solution (Mag. = 10 KX).

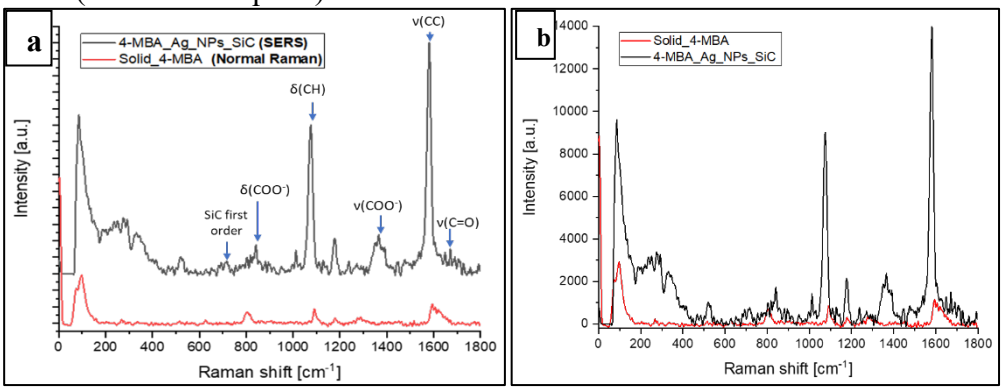

Fig. 3. a) SERS spectrum of 4-MBA molecules at 1 x 10^{-5}M, on AgNPs_SiC plasmonic substrate (black line) superimposed on Normal Raman spectrum of solid 4-MBA (red line) acquired in the same conditions. b) Comparison of peak intensities of spectra obtained from SERS (black line) and Normal Raman (red line) analysis.

Raman analysis were conducted using a 532 nm laser ʎ which is close to ω of silver [27]. For each sample, four Raman acquisitions were performed, at different points, to verify the signal reproducibility.

SERS of 4-MBA on Ag NPs and Normal Raman of solid 4-MBA spectra are reported in Fig. 3 a) and b). The most intense peak of 4-MBA is found at 1590 cm^{-1}, corresponding to aromatic-ring breathing modes and its intensity is used for determining the EF. The other characteristic peaks are shown in Table 1 [28]. At 797 cm^{-1} the peak corresponding to the first-order transverse optic (TO) of 4H-SiC is observable. In relation to the local environment the dielectric function changes and therefore the resonance condition occurs for different wavelengths [29]. In fact, comparing the spectra in Fig. 3 it is visible a red-shift of the 4-MBA bands in SERS spectrum with respect to the same peaks in the Normal Raman spectrum. To assess EF, a rough estimation of the amount of 4-MBA bound to Ag NPs was obtained by UV-VIS absorption spectroscopy, by measuring the absorbance spectra of the 1 $x10^{-5}$ M solution of 4-MBA before (Fig. 4, black line) and after immersion of the sample (Fig. 4, red line). The blue line in Fig. 4 represents the signal obtained from the subtraction of the two spectra. From this signal it is possible to estimate the concentration of the molecules coating the NPs by applying the well Lambert-Beer law:

Table 1. Vibrational band $[cm^{-1}]$ of 4-MBA.

Typical Raman bands of 4-MBA:	
Vibrational mode	Raman shift $[cm^{-1}]$
γ(CCC)	720
δ(COO^-)	846
β(SH)	915
δ(CH)	1075
ν(COO^-)	1370
ν(CC)	1590
ν(C=O)	1710
ν(SH)	2550

$$A=\varepsilon dC. \tag{2}$$

where A is absorbance; ε is the molar absorption coefficient, d is the optical path length and C is the molecules concentration [30]. Analytical EF (AEF) is:

$$AEF = \frac{I_{SERS}/C_{SERS}}{I_{NR}/C_{NR}} \cong 6{,}3 \times 10^{7}. \tag{3}$$

Where I_{SERS} and I_{NR} are the intensities of 1590 cm^{-1} peak for SERS and Normal Raman spectra, respectively, while C_{SERS} is the calculated concentration of 4-MBA on the substrate (1,9 x 10^{-6} M) and C_{NR} is the solid 4-MBA concentration, taken as unity [31]. When the sample is pulled out from solution, multiple layers of 4-MBA are deposited on the Ag NPs, which are then removed by rinsing in ethanol. Thus, obtained EF value is underestimate with respect to its real value, as the C_{SERS} obtained is greater than the real one.

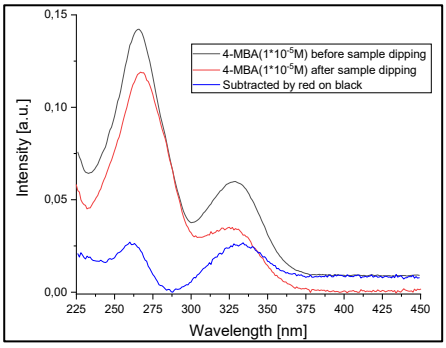

Fig. 4 Absorption spectra of 1 x 10^{-5} M solution of 4-MBA, before (black line) and after (red line) dipping of plasmonic substrate. Blue line is spectrum obtained from the two spectra subtraction.

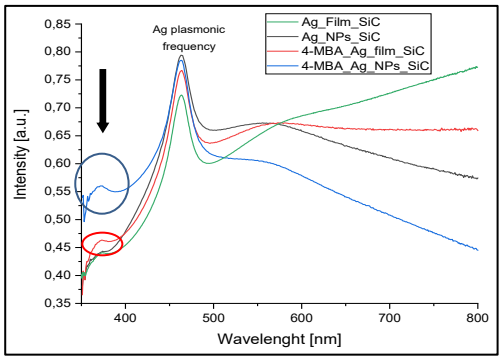

Fig. 5 Absorption spectra of: Ag film on SiC (green); Ag NPs on SiC (black); 4-MBA on Ag_film_SiC (red) and 4-MBA on Ag_NPs_SiC (blue).

For design of portable integrated optical sensor, Raman spectroscopy is certainly not suitable, as it requires a complex and expensive apparatus. An interesting approach could be UV-Vis spectroscopy. In this perspective, the UV-Vis analysis, shown in Fig. 5, of previously described samples, Ag_film_SiC (green line), Ag_NPs_SiC (black line), 4-MBA_Ag_film_SiC (red line) and 4-MBA_Ag_NPs_SiC (blue line), without further modification, were performed to test whether the binding of 4-MBA produces changes in the extinction spectrum of Ag_NPs_SiC plasmonic substrate. Extinction are affected by the UV absorption of the 4H-SiC substrate, at 380 nm. of substrate. By comparing #Ag_film_SiC and #Ag_NPs_SiC spectra, as expected, silver plasmon resonance peak, at about 460 nm, is more intense for the latter. While the spectral pattern of the substrate in the two samples is very similar. In the absorption spectra of #4-MBA_Ag_film_SiC (red line) and #4-MBA_Ag_NPs_SiC (blue line), we observe a shoulder band around 360-370 nm, which is more intense when 4-MBA is bound to the Ag NPs (blue circle) than to the film (red circle), due to the plasmonic effect. This relevant modification in the absorbance signals can be used as diagnostic for target molecule monitoring.

A possible sensing system is sketched in Fig. 6 consisting of: a photon source emitting at the desired ʎ, in front of an optical sensor NPs based. The sensor could consists in an detector (such as a SiC UV photodiode) covered by an opportune, electrically insulated, plasmonic structure (such as MNPs) suitably functionalized to favor selective binding to the chemical species of interest directly exposed to the optical source [30–32]. The optical signal, is partially absorbed by the plasmonic Ag NPs structures binding the species of interest and is then detected by the bottom optical photodiode. The optical operating range is related to the band gap of the semiconductor used. Among the WBG semiconductors, 3C-SiC, due to its band gap value (2.45 eV corresponding to about 517 nm), could be a promising candidate for monitoring organic substances, whose optical absorption falls between 300 and 500 nm. Moreover, the possibility to growth 3C-polytype on silicon substrate, represents a great advantage both economically and technologically for low cost integrated sensing system.

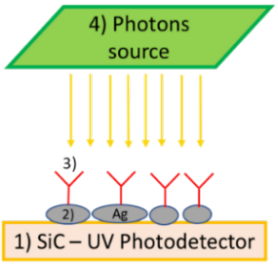

Fig. 6 Schematic of sensor: Ag NPs 2) on SiC 1), suitably functionalised 3). Light emitted by a photon source 4) reaches the Ag NPs and the transmitted component is detected by the SiC UV photodetector 1).

Conclusion

A plasmonic substrate consisting of Ag NPs, obtained by SSD of an Ag thin film on SiC substrate was studied. 4-MBA probe molecule was adhered to the substrate, which was subsequently revealed by SERS and UV-Vis Spectroscopy. As a substrate for SERS it was shown to produce a Raman signal enhancement of more than 10^7. The Absorbance spectrum showed a new shoulder band between 360 and 370 nm when 4-MBA was bound on Ag NPs. A portable integrated bio-chemical sensor can be obtained integrating NPs on SiC UV photodiode. We propose a device with suitably functionalized Ag NPs picking up the molecules of interest and producing a relevant changes of optical transmitted signal, detected by underlying SiC active device. Moreover the effect of SiC different termination (C or Si) on dewetting phenomenon will be investigated.

References

[1] X. Wang, et al. , Physical Chemistry Chemical Physics, vol. 14, no. 17. pp. 5891–5901, 2012.

[2] S. Nie and S. R. Emory, Science (80-.)., vol. 275, no. 5303, pp. 1102–1106, 1997.

[3] T. Y. Jeon, D. J. Kim, S. G. Park, S. H. Kim, and D. H. Kim, Nano Convergence, vol. 3, no. 1. 2016.

[4] K. H. Leong, H. Y. Chu, S. Ibrahim, and P. Saravanan, pp. 428–437, 2015, doi: 10.3762/bjnano.6.43.

[5] P. J. Andrew Wilson, ACS Publ., 2020.

[6] J. Krajczewski, K. Kołątaj, and A. Kudelski, RSC Advances, vol. 7, no. 28. 2017.

[7] M. A. Garcia, Journal of Physics D: Applied Physics, vol. 44, no. 28. 2011.

[8] H. K. Lee et al., Chem. Soc. Rev., vol. 48, no. 3, pp. 731–756.

[9] K. Shrivas, R. Shankar, and K. Dewangan, Sensors Actuators, B Chem., vol. 220, 2015.

[10] S. Rasheed, et al., J. Ind. Eng. Chem., no. xxxx, 2023.

[11] W. Jia, E. P. Douglas, F. Guo, and W. Sun, Appl. Phys. Lett., vol. 85, no. 26, pp. 6326–6328, 2004.

[12] M. Turino, et al., RSC Adv., vol. 12, no. 2, pp. 845–859, 2022.

[13] L. Guerrini and R. A. Alvarez-Puebla, ACS Omega, vol. 6, no. 2, pp. 1054–1063, 2021.

[14] L. Guerrini, et al., Cancers (Basel)., vol. 13, no. 9, pp. 1–28, 2021.

[15] D. Cialla et al., Anal. Bioanal. Chem., vol. 403, no. 1, pp. 27–54, 2012.

[16] C. Wang et al., AIP Adv., vol. 9, no. 1, 2019.

[17] J. N. Anker, , Nat. Mater., vol. 7, no. June, pp. 8–10, 2008.

[18] C. V. Thompson, Annual Review of Materials Research, vol. 42. 2012.

[19] A. Araújo et al., J. Phys. Chem. C, vol. 120, no. 32, pp. 18235–18242, Aug. 2016.

[20] S. J. Randolph et al., Nanotechnology, vol. 18, no. 46, 2007.

[21] C. M. Müller and R. Spolenak, Acta Mater., vol. 58, no. 18, 2010.

[22] A. L. Giermann and C. V. Thompson, Appl. Phys. Lett., vol. 86, no. 12, 2005.

[23] T. Seyller, Appl. Phys. A Mater. Sci. Process., vol. 85, no. 4, pp. 371–385, 2006.

[24] A. Brancato et al., Surfaces and Interfaces, vol. 40, no. July, 2023, doi: 10.1016/j.surfin. 2023.103157.

[25] P. Reokrungruang, et al., Sensors Actuators, B Chem., vol. 285, October 2018, pp. 462–469, 2019.

[26] C. Novara et al., RSC Adv., vol. 6, no. 26, pp. 21865–21870, 2016.

[27] K. Khurana and N. Jaggi, Plasmonics, vol. 16, no. 4, pp. 981–999, 2021.

[28] C. J. Orendorff, et al., Anal. Chem., vol. 77, no. 10, pp. 3261–3266, 2005.

[29] X. Zhang, Y. L. Chen, R. S. Liu, and D. P. Tsai, Reports Prog. Phys., vol. 76, no. 4, 2013.

[30] W. Mäntele and E. Deniz, SAA, vol. 173, pp. 965–968, 2017, doi: 10.1016/j.saa.2016.09.037.

[31] E. C. Le Ru and P. G. Etchegoin, MRS Bull., vol. 38, no. 8, pp. 631–640, 2013.

[32] A. Sciuto et al., IEEE Photonics J., vol. 9, no. 1, 2017.

[33] A. Sciuto, et al., IEEE Photonics Technol. Lett., vol. 26, no. 17, pp. 1782–1785, 2014.

[34] “patent System and method for detecting the concentration of metal particles.pdf.” .